

Angular dependence of pinning potential, upper critical field, and irreversibility field in underdoped BaFe_{1.9}Co_{0.1}As₂ single crystal

M. Shahbazi, X. L. Wang, S. R. Ghorbani, S. X. Dou, and K. Y. Choi

Citation: [Applied Physics Letters](#) **100**, 102601 (2012); doi: 10.1063/1.3692582

View online: <http://dx.doi.org/10.1063/1.3692582>

View Table of Contents: <http://scitation.aip.org/content/aip/journal/apl/100/10?ver=pdfcov>

Published by the [AIP Publishing](#)

Articles you may be interested in

[Superconductivity in BiS₂ based Bi₄O₄S₃ novel compound](#)

[AIP Conf. Proc.](#) **1512**, 1104 (2013); 10.1063/1.4791432

[Flux pinning and vortex transitions in doped BaFe₂As₂ single crystals](#)

[Appl. Phys. Lett.](#) **100**, 072603 (2012); 10.1063/1.3685507

[Enhancement of the upper critical field in codoped iron-arsenic high-temperature superconductors](#)

[J. Appl. Phys.](#) **110**, 123906 (2011); 10.1063/1.3665700

[Magnetoresistance, critical current density, and magnetic flux pinning mechanism in nickel doped BaFe₂As₂ single crystals](#)

[J. Appl. Phys.](#) **109**, 07E151 (2011); 10.1063/1.3563057

[Small anisotropy, weak thermal fluctuations, and high field superconductivity in Co-doped iron pnictide Ba \(Fe 1 - x Co x \) 2 As 2](#)

[Appl. Phys. Lett.](#) **94**, 062511 (2009); 10.1063/1.3081455

An advertisement for COMSOL Multiphysics simulation projects. The background is dark with a grid pattern. On the left, there is a 3D cutaway view of a mechanical part with a red and yellow color gradient. The text 'Over 600 Multiphysics Simulation Projects' is prominently displayed in white and blue. A blue button with white text 'VIEW NOW >>' is located on the right. The COMSOL logo is in the bottom right corner.

Over **600** Multiphysics Simulation Projects

[VIEW NOW >>](#)

COMSOL

Angular dependence of pinning potential, upper critical field, and irreversibility field in underdoped BaFe_{1.9}Co_{0.1}As₂ single crystal

M. Shahbazi,¹ X. L. Wang,^{1,a)} S. R. Ghorbani,^{1,2} S. X. Dou,¹ and K. Y. Choi³

¹*Institute for Superconducting and Electronic Materials, Faculty of Engineering, Australian Institute for Innovative Materials, University of Wollongong, North Wollongong, NSW 2519, Australia*

²*Department of Physics, Sabzevar Tarbiat Moallem University, P.O. Box 397, Sabzevar, Iran*

³*Frontier Physics Research Division and Department of Physics and Astronomy, Seoul National University, Seoul 151-747, South Korea*

(Received 1 December 2011; accepted 19 February 2012; published online 7 March 2012)

Underdoped BaFe_{1.9}Co_{0.1}As₂ single crystal was studied by angular dependence of magneto-transport at fields up to 13 T over a wide range of temperature. Our results show that pinning potential, U_0 , decreases slightly for $\theta \leq 45^\circ$ and remains constant for $\theta \geq 45^\circ$, while the upper critical field, H_{c2} , and the irreversibility field, H_{irr} , increase with θ . According to anisotropic Ginzburg-Landau theory, the anisotropy was determined by scaling the resistivity under different magnetic fields below the superconducting critical temperature, T_c . Anisotropy, Γ , in the underdoped crystal is found to be temperature dependent and decreases from 2.1 to 1.8 for as T is reduced from 17 to 12.5 K. © 2012 American Institute of Physics. [<http://dx.doi.org/10.1063/1.3692582>]

The thermal activation behaviour of vortices in superconductors determines their magneto-transport properties, which are critical for practical applications. In highly anisotropic cuprates, a magnetic field perpendicular to the superconducting layers penetrates in the form of pancake vortices, while a parallel field creates Josephson vortices.¹ The interaction between pancake vortices and Josephson vortices creates vortex chains² or Josephson vortices decorated by pancake vortices³ when the magnetic field is tilted. The pinning potential in cuprates is highly anisotropic and strongly field dependent due to the strong thermally activated behaviour of two-dimensional (2D) pancake vortices.

Iron based superconductors⁴ exhibit relatively high transition temperature, T_c , very high upper critical field,⁵ H_{c2} , and relatively low anisotropy.⁶⁻⁹ Among pnictide superconductors, Ba-122 compounds have typical 2D layered crystal structure. However, they show nearly isotropic superconductivity⁶ and very high intrinsic pinning potential, which is weakly field dependent.¹⁰ These unique features make the 122 superconductors more favourable for practical application than other pnictide superconductors.

Thermally activated flux flow has been studied in NdFeAsO_{0.7}F_{0.3},¹¹ Ba_{0.72}K_{0.28}Fe₂As₂,¹⁰ BaFe_{1.9}Ni_{0.1}As₂,¹² and Tl_{0.58}Rb_{0.42}Fe_{1.72}Se₂ (Ref. 13) single crystals for $H//ab$ and $H//c$. Very recently, studies of the angular dependence of the transport critical current density, J_c , have indicated that the J_c decreases monotonically with angle, θ , for $\theta < 90^\circ$, where θ is defined as the angle between the magnetic field and the c -axis. The ratio of $J_c(H//ab)/J_c(H//c) = 7.5$ or 1.8 at $H = 1$ T and $T = 4.2$ K for La-1111 (Ref. 14) and Co-122 (Ref. 15) thin film, respectively. It should be noted that the determination of the angular dependence of the pinning potential, H_{c2} , and the irreversibility field, H_{irr} , are important for understanding how J_c changes with both

angle and field. So far, there has been no report on the angular dependence of these parameters in any pnictide superconductors. In this letter, we report the angular dependence of the upper critical field, the irreversibility field, and the pinning potential of underdoped BaFe_{1.9}Co_{0.1}As₂ single crystal by measuring magneto-transport at different magnetic fields and angles. Furthermore, by scaling the angular dependence of the resistance, based on the anisotropic Ginzburg-Landau (GL) theory, the anisotropy value (Γ) was determined for different temperatures. Our results show that the pinning potential, U_0 , is strongly angle dependent for $\theta \leq 45^\circ$ and almost angle independent for $\theta \geq 45^\circ$, while both H_{c2} and H_{irr} increase monotonically with increasing angle.

The single crystal of BaFe_{1.9}Co_{0.1}As₂ was grown using the high temperature self-flux method. FeAs and CoAs were prepared by placing a mixture of As powder and Fe/Co powder in a quartz tube and reacting it at 600 °C for 10 h after it had been heated to 600 °C for 17 h. A mixture of FeAs/CoAs and Ba pieces was then placed in an alumina crucible. The whole assembly was sealed in a large quartz tube and heated to 1180 °C for 15 h, which was followed by a reaction at 1180 °C for 10 h.¹⁶ The as-grown single crystal was cleaved and cut into a rectangular shape for measurements. The transport properties were measured over a wide range of temperature and magnetic fields up to 13 T with applied current of 5 mA, using a physical properties measurement system (PPMS, quantum design). The current was applied in the ab plane. The angular dependence of the resistivity was measured using the 13 T PPMS, with the angle, θ , varied from 0° to 180°, where $\theta = 0^\circ$ corresponded to the configuration of $H//c$ and $\theta = 90^\circ$ to $H//ab$, respectively.

The temperature dependence of the in-plane resistivity of the underdoped BaFe_{1.9}Co_{0.1}As₂ single crystal is shown in Fig. 1. The resistivity decreases with decreasing temperature from 300 K to 50 K, supporting metallic behaviour of this compound. The resistivity increases with further decreasing temperature and shows an anomaly at 49 K due to a

^{a)}Author to whom correspondence should be addressed. Electronic mail: xiaolin@uow.edu.au.

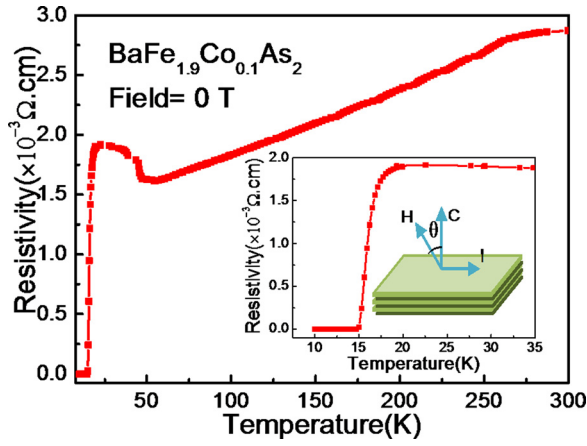


FIG. 1. (Color online) Temperature dependence of the in-plane resistivity of $\text{BaFe}_{1.9}\text{Co}_{0.1}\text{As}_2$. The inset shows an enlargement of the region with $T \leq 35$ K and a schematic diagram of the sample.

magnetic/structural phase transition.¹⁷ The T_c^{onset} and $T_c(0)$ were determined to be 17.4 and 15.2 K, respectively.

The angular dependence of the resistance at $T = 17$ K is shown in Figure 2(a). All the curves show a symmetric dip-like structure, with a minimum at 90° and maximum resistance at 0° and 180° . The normal state resistance decreases with decreasing magnetic field and temperature, due to the enhancement of the superconducting state. The angular dependence of resistance is not very sharp with varying field and temperature, possibly due to the moderate anisotropy of the $\text{BaFe}_{1.9}\text{Co}_{0.1}\text{As}_2$ sample, which has also been reported in Nd-1111 single crystals.¹⁸ Similar behaviour observed at $T = 15$ and 12.5 K.

In layered superconductors, the variation in the superconducting order parameter, ψ , can be described by $\delta\Psi/\delta z$ when the order parameter is quasi-continuous across the neighbouring layers. Therefore, the anisotropic Ginzburg-Landau approximation, $H_{c2}^{ab}/\sqrt{\sin^2\theta + \Gamma^2\cos^2\theta}$, can be used to estimate the anisotropy values for our sample. The angular dependence of the resistance can be scaled as $R = R(0)f(H/H_{c2}^{GL})$.¹⁹ Then, the resistance measured under different magnetic fields should collapse into one curve at a certain temperature if the Γ parameter is properly scaled. The results of this scaling at $T = 17$ K is shown in Figure 2(b). The estimated anisotropy value, is 1.8 for $T = 12.5$ K, 1.9 for $T = 15$ K, and 2.1 for $T = 17$ K. The obtained anisotropy values are very close to the reported value of 2 at $T = T_c$ for $\text{BaFe}_{2-x}\text{Co}_x\text{As}_2$ single crystals.²⁰ The anisotropy values which are obtained from this rescaling analysis are more reli-

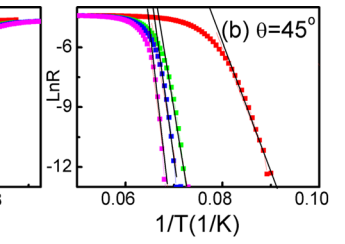
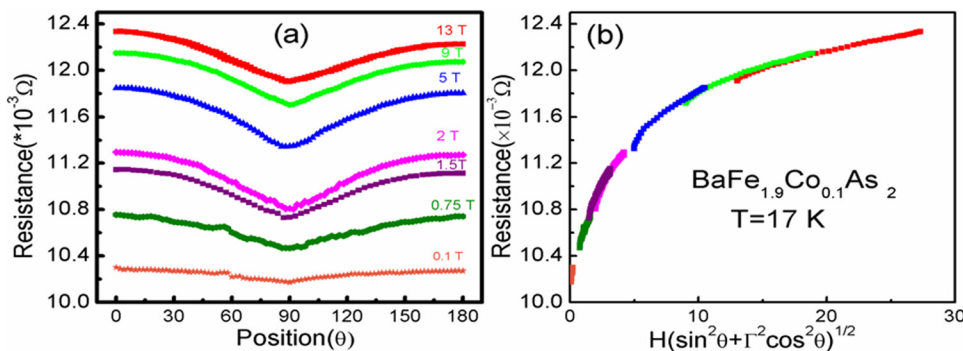


FIG. 3. (Color online) (a) Temperature dependence of resistance at different magnetic fields for $\theta = 45^\circ$ where θ is the angles between the applied magnetic field and the c -axis. (b) Arrhenius plots of the resistivity at the same angles in underdoped $\text{BaFe}_{1.9}\text{Co}_{0.1}\text{As}_2$ single crystal.

able compared to estimating the anisotropy using the ratio of H_{c2} in the ab plane to that along the c -axis.

The results of magneto-transport measurements at $\theta = 45^\circ$ is shown in Fig. 3(a) where θ is the angles between the applied magnetic field and the c -axis. According to the thermally activated flux flow model, the resistance can be described as

$$R = (2v_0LH/J)\sinh\left[\frac{JHVL}{T}\right]e^{i_cHVL/T}, \quad (1)$$

where v_0 is the attempt frequency for flux bundle hopping, L is the hopping distance, J is the applied current density, J_{c0} is the critical current density at 0 T, and V is the bundle volume.²¹ If $JHVL/T \ll 1$, Eq. (1) can be written as

$$R = (2R_cU/T)e^{-U/T}, \quad (2)$$

where $U = J_{c0}HVL$ is the thermally activated energy and the critical resistance, $R_c = v_0LH/J_{c0}$. Assuming that $2R_cU/T$ is a temperature independent constant, defined as R_0 and $U = U_0(1-T/T_c)$ then Eq. (2) can be simplified as the Arrhenius equation

$$\ln R(T, H) = \ln R_0 - U_0/T,$$

Therefore, the activation energy, $U_0(B)$, is the slope of the lower part of the curve in the Arrhenius plot.

In order to study the flux motion in $\text{BaFe}_{1.9}\text{Co}_{0.1}\text{As}_2$ single crystal, we plot the electrical resistance as a function of $1/T$ at different magnetic fields up to 7 T and different angles between the applied magnetic field and the c -axis. Fig. 3(b) shows the Arrhenius plot of the resistance for $\theta = 45^\circ$. The linear dependence of $\ln R$ on $1/T$ in the lower part of the curves indicates that this part can be described by the thermally

FIG. 2. (Color online) (a) The angular dependence of the magnetoresistance at $T = 17$ K. (b) Scaling of the resistance as a function of $H(\sin^2\theta + \Gamma^2\cos^2\theta)^{1/2}$ based on GL theory at $T = 17$ K.

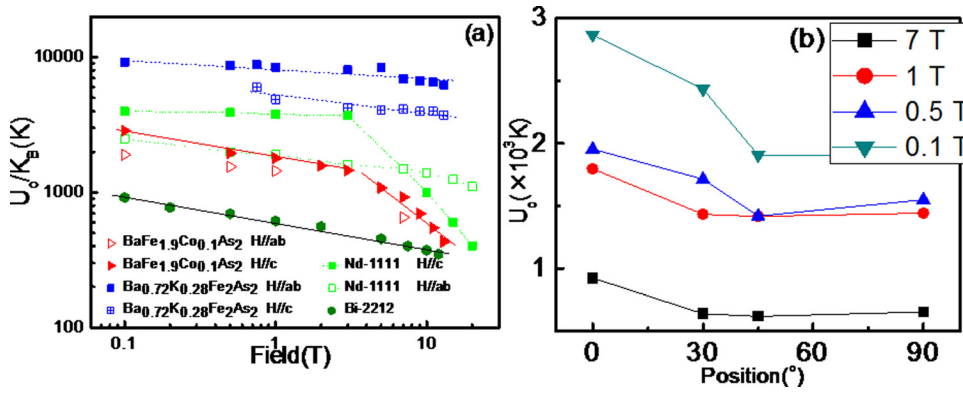


FIG. 4. (a) (Color online) Field dependence of U_0 for $\text{BaFe}_{1.9}\text{Co}_{0.1}\text{As}_2$ single crystal. (b) Angular dependence of pinning potential for different magnetic fields.

activated flux flow model.¹¹ Similar measurements were performed for several other angles, from 0° up to 90°, and $U_0(B)$ was calculated from the corresponding Arrhenius plots.

Fig. 4(a) shows the magnetic field dependence of U_0 for H//c and H//ab in underdoped $\text{BaFe}_{1.9}\text{Co}_{0.1}\text{As}_2$ single crystal. The best fit of the experimental data yields pinning potential values ranging from $U_0/k_B = 2900$ K to 1900 K, where k_B is the Boltzmann constant, for H//c and H//ab, respectively, at the low magnetic field of 0.1 T. These values are comparable to the reported values of $U_0 = 3000$ –4000 K for $\text{NdFeAsO}_{0.82}\text{F}_{0.18}$ single crystals.¹¹ For comparison, we also included the U_0 for Bi-2212 single crystal in Fig. 4(a). The U_0 value for underdoped $\text{BaFe}_{1.9}\text{Co}_{0.1}\text{As}_2$ is three times higher than for Bi-2212 single crystal.²² However, this value is lower than the reported value of 9100 K for $\text{Ba}_{0.72}\text{K}_{0.28}\text{Fe}_2\text{As}_2$ single crystal¹⁰ for H//ab. The U_0 value for our underdoped $\text{BaFe}_{1.9}\text{Co}_{0.1}\text{As}_2$ crystal with H//c exhibits a weak power-law dependence ($U_0 \propto H^{-0.15}$) for $H < 3$ T, where single vortex pinning dominates, followed by a power-law decrease with $U_0 \propto H^{-0.81}$, indicating collective pinning at higher fields, $H > 3$ T. The pinning potential values decrease when the sample is rotated from H//c to H//ab. It should be noted that the U_0 decreases slightly for $0 < \theta \leq 45^\circ$, and then remains constant for $\theta \geq 45^\circ$ (Fig. 4(b)). Possibly, twin boundaries which can form below the temperature of the structural transition from tetragonal to

orthorhombic could act as barriers to vortex motion, resulting in the higher U_0 value for H//c (Refs. 23 and 24) compared to that for H//ab.

The critical current density, J_c , vs. magnetic field is shown in Fig. 5(a). J_c was calculated from the magnetic hysteresis data at $T = 2$ and 4.2 K by using the extended Bean model

$$J_c = 20 \times \Delta M / V / (a(1 - a/3b)) \quad \text{with } a < b,$$

where a and b are the sample dimensions, V is the sample volume, and ΔM is the height of the magnetization loop. The J_c is as high as 1.7×10^5 and 1.5×10^5 A/cm² at $T = 2$ and 4.2 K in zero magnetic fields, respectively. The J_c decreases with increasing magnetic field up to 1 T and after that become nearly field independent which is related to relatively high pinning potential and weakly anisotropic property in $\text{BaFe}_{1.9}\text{Co}_{0.1}\text{As}_2$ single crystal.

The upper critical field, H_{c2} , is characterized as the field at which the resistivity becomes 90% of the normal state resistivity; while the irreversibility field, H_{irr} , is defined by 10% of the normal state resistivity. Figure 5(b) shows H_{c2} and H_{irr} as functions of temperature for different angles between the field and the c -axis. From Fig. 5(c), the H_{c2} and H_{irr} follow the same trend with angle for $\theta > 45^\circ$. The estimated slopes dH_{c2}^{ab}/dT and dH_{irr}^{ab}/dT are 4.8 and 3.79 T/K for H//ab. The dH_{c2}^{ab}/dT is in good agreement with the reported value of $dH_{c2}^{ab}/dT = 4.9$ T/K.²⁰ The slopes decrease as the sample is rotated from 0° to 90° (Fig. 5(d)), which is similar to the trend of U_0 with angle.

In summary, we have investigated the angular dependence of U_0 , H_{c2} , and H_{irr} for underdoped $\text{BaFe}_{1.9}\text{Co}_{0.1}\text{As}_2$ single crystal. U_0 decreases while H_{c2} and H_{irr} increase with angle from H//c to H//ab. The anisotropy parameter decreased from 2.1 to 1.8 as T decreased from 17 to 12.5 K, using the anisotropic GL theory.

This work is supported by the Australian Research Council (ARC) through Discovery Projects DP 1094073 and DP0558753.

¹L. Bulaevskii and J. R. Clem, *Phys. Rev. B* **44**, 10234 (1991).

²A. E. Koshelev, *Phys. Rev. B* **71**, 174507 (2005).

³A. Grigorenko, S. Bending, T. Tamegai, S. Ooi, and M. Henini, *Nature* **414**, 728 (2001).

⁴Y. Kamihara, T. Watanabe, M. Hirano, and H. Hosono, *J. Am. Chem. Soc.* **130**, 3296 (2008).

⁵F. Hunte, J. Jaroszynski, A. Gurevich, D. C. Larbalestier, R. Jin, A. S. Sefat, M. A. McGuire, B. C. Sales, D. K. Christen, and D. Mandrus, *Nature* **453**, 903 (2008).

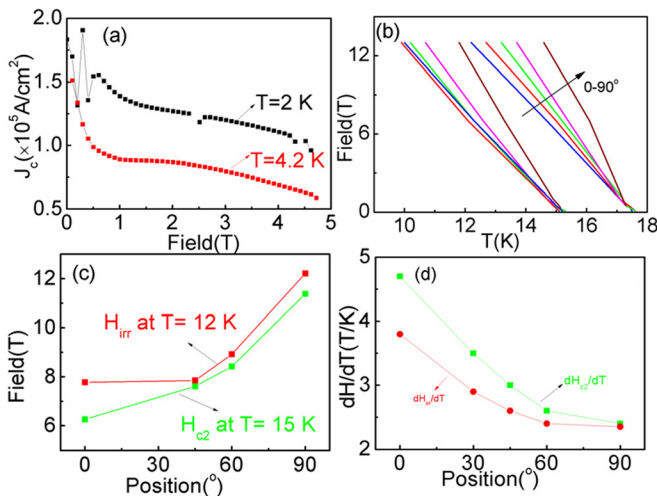


FIG. 5. (a) (Color online) Field dependence of J_c at $T = 2$ and 4.2 K. (b) Angular dependence of H_{c2} and H_{irr} as a function of temperature. (c) Angular dependence of H_{c2} and H_{irr} at fixed temperature. (d) Angular dependence of dH_{c2}/dT and dH_{irr}/dT .

- ⁶H. Q. Yuan, J. Singleton, F. F. Balakirev, S. A. Baily, G. F. Chen, J. L. Luo, and N. L. Wang, *Nature* **457**, 565 (2009).
- ⁷N. Ni, M. E. Tillman, J. Q. Yan, A. Kracher, S. T. Hannahs, S. L. Bud'ko, and P. C. Canfield, *Phys. Rev. B* **78**, 214515 (2008).
- ⁸M. M. Altarawneh, K. Collar, C. H. Mielke, N. Ni, S. L. Bud'ko, and P. C. Canfield, *Phys. Rev. B* **78**, 220505 (2008).
- ⁹M. A. Tanatar, N. Ni, C. Martin, R. T. Gordon, H. Kim, V. G. Kogan, G. D. Samolyuk, S. L. Bud'ko, P. C. Canfield, and R. Prozorov, *Phys. Rev. B* **79**, 094507 (2009).
- ¹⁰X.-L. Wang, S. R. Ghorbani, S.-I. Lee, S. X. Dou, C. T. Lin, T. H. Johansen, K.-H. Müller, K. H. Iler, Z. X. Cheng, G. Peleckis *et al.*, *Phys. Rev. B* **82**, 024525 (2010).
- ¹¹J. Jaroszynski, F. Hunte, L. Balicas, Y.-j. Jo, I. Raiccaronevicacuta, A. Gurevich, D. C. Larbalestier, F. F. Balakirev, L. Fang, P. Cheng, Y. Jia *et al.*, *Phys. Rev. B* **78**, 174523 (2008).
- ¹²M. Shahbazi, X. L. Wang, Z. W. Lin, J. G. Zhu, S. X. Dou, and K. Y. Choi, *J. Appl. Phys.* **109**, 07E151 (2011).
- ¹³L. Jiao, Y. Kohama, J. L. Zhang, H. D. Wang, B. Maiorov, F. F. Balakirev, Y. Chen, L. N. Wang, T. Shang, M. H. Fang *et al.*, *Phys. Rev. B* **85**, 064513 (2012).
- ¹⁴M. Kidszun, S. Haindl, T. Thersleff, J. Hänisch, A. Kauffmann, K. Iida, J. Freudenberger, L. Schultz, and B. Holzapfel, *Phys. Rev. Lett.* **106**, 137001 (2011).
- ¹⁵K. Iida, J. Hänisch, T. Thersleff, F. Kurth, M. Kidszun, S. Haindl, R. Hühne, L. Schultz, and B. Holzapfel, *Phys. Rev. B* **81**, 100507 (2010).
- ¹⁶S. H. Kim, C. H. Choi, M.-H. Jung, J.-B. Yoon, Y.-H. Jo, X. F. Wang, X. H. Chen, X. L. Wang, S.-I. Lee, and K.-Y. Choi, *J. Appl. Phys.* **108**, 063916 (2010).
- ¹⁷J.-H. Chu, J. G. Analytis, C. Kucharczyk, and I. R. Fisher, *Phys. Rev. B* **79**, 014506 (2009).
- ¹⁸Y. Jia, P. Cheng, L. Fang, H. Yang, C. Ren, L. Shan, C.-Z. Gu, and H.-H. Wen, *Supercond. Sci. Technol.* **21**, 105018 (2008).
- ¹⁹G. Blatter, V. B. Geshkenbein, and A. I. Larkin, *Phys. Rev. Lett.* **68**, 875 (1992).
- ²⁰A. Yamamoto, J. Jaroszynski, C. Tarantini, L. Balicas, J. Jiang, A. Gurevich, D. C. Larbalestier, R. Jin, S. Sefat, M. A. McGuire *et al.*, *Appl. Phys. Lett.* **94**, 062511 (2009).
- ²¹G. Blatter, M. V. Feigel'man, V. B. Geshkenbein, A. I. Larkin, and V. M. Vinokur, *Rev. Mod. Phys.* **66**, 1125 (1994).
- ²²T. T. M. Palstra, B. Batlogg, R. B. van Dover, L. F. Schneemeyer, and J. V. Wasczak, *Phys. Rev. B* **41**, 6621 (1990).
- ²³B. Kalisky, J. R. Kirtley, J. G. Analytis, J. H. Chu, I. R. Fisher, and K. A. Moler, *Phys. Rev. B* **83**, 064511 (2011).
- ²⁴B. Kalisky, J. R. Kirtley, J. G. Analytis, J.-H. Chu, A. Vailionis, I. R. Fisher, and K. A. Moler, *Phys. Rev. B* **81**, 184513 (2010).